HHS Public Access

Author manuscript

Nat Immunol. Author manuscript; available in PMC 2013 August 01.

Published in final edited form as:

Nat Immunol. 2013 February ; 14(2): 136–142. doi:10.1038/ni.2508.

Parasite-induced T_H1 cells and intestinal dysbiosis cooperate in IFN-γ-dependent elimination of Paneth cells

Megan Raetz[1], **Sun-hee Hwang**[1], **Cara Wilhelm**[1], **Donna Kirkland**[1], **Alicia Benson**[1], **Carolyn Sturge**[1], **Julie Mirpuri**[1], **Shipra Vaishnava**[1], **Baidong Hou**[2,3], **Anthony L. DeFranco**[2], **Christopher J Gilpin**[4], **Lora V. Hooper**[1,5], and **Felix Yarovinsky**[1,*]

[1]Department of Immunology, University of Texas Southwestern Medical Center, Dallas, TX, 75390

[2]Department of Microbiology & Immunology, University of California, San Francisco, CA, 94143

[3]Key Laboratory of Infection and Immunity, Institute of Biophysics, Chinese Academy of Sciences, Beijing, China

[4]Department of Cell Biology, University of Texas Southwestern Medical Center, Dallas, TX, 75390

[5]The Howard Hughes Medical Institute

Abstract

Activation of Toll-like receptors (TLRs) by pathogens triggers cytokine production and T cell activation, immune defense mechanisms that are linked to immunopathology. Here we show that IFN-γ production by $CD4^+$ T_H1 cells during mucosal responses to the protozoan parasite *Toxoplasma gondii* results in dysbiosis and the elimination of Paneth cells. Paneth cell death led to loss of antimicrobial peptides and occurred in conjunction with uncontrolled expansion of the *Enterobacteriaceae* family of Gram-negative bacteria. The expanded intestinal bacteria were required for the parasite-induced intestinal pathology. The investigation of cell type-specific factors regulating T_H1 polarization during *T. gondii* infection identified the T cell intrinsic TLR pathway as a major regulator of IFN-γ production in $CD4^+$ T cells responsible for Paneth cell death, dysbiosis and intestinal immunopathology.

Microbial and viral infections result in the potent activation of the innate and adaptive immune cells required for host resistance to pathogens[1–3]. Multiple classes of receptors are involved in the early detection of pathogens and the regulation of immunity. In most cases, the activation of Toll-like receptors (TLR) triggers inflammatory programs dependent on the adaptor MyD88[1]. Impaired TLR- and MyD88-dependent sensing of pathogens results in increased susceptibility to microbial and viral infections caused by uncontrolled pathogen dissemination[1–3]. Inflammation driven by TLR pathway activation can also lead to severe and sometimes lethal tissue damage[4]. The beneficial and detrimental effects of TLR-driven

*Correspondence to: felix.yarovinsky@UTSouthwestern.edu.

inflammation in the context of infectious diseases are particularly evident during immune responses to the protozoan parasite *Toxoplasma gondii*[5]. *T. gondii*-infected wild-type mice initiate potent interleukin 12 (IL- 12)-dependent interferon-γ (IFN-γ) responses, which are impaired by MyD88 inactivation[6,7]. As a result, mice deficient in MyD88 succumb due to uncontrolled parasite dissemination, with kinetics and pathogen loads that are practically indistinguishable from those seen in IL-12 and IFN-γ-deficient mice[8–10]. However, overproduction of IFN-γ in response to the same pathogen in mice unable to produce the immunoregulatory cytokine IL-10 also leads to rapid death, despite efficient control of the pathogen[11,12]. Severe tissue damage caused by IFN-γ seems to be responsible for the death of IL-10-deficient mice infected with *T. gondii*[13]. Thus, while IFN-γ-expressing T_H1 cells play an indispensable role in host resistance, these cells can also cause tissue destruction and lethal immunopathology. Furthermore, even in wild-type mice, mucosal responses to the parasite result in detrimental T_H1 cell-driven intestinal pathology[14]. Despite a well-appreciated role for MyD88 in driving T_H1 responses against the parasite[15,16] and identification of TLR11 as a major activator of MyD88 during murine toxoplasmosis[17], little is known about cell type-specific MyD88-dependent programs dictating T_H1 polarization *in vivo*[16]. Such insight is essential for understanding the mechanisms regulating T_H-mediated host protection and the factors responsible for $CD4^+$ T cell-associated immunopathology. Here we identified that IFN-γ production by $CD4^+$ T_H1 cells during mucosal responses to the protozoan parasite *Toxoplasma gondii* is regulated by T cell intrinsic MyD88 signaling pathway. $CD4^+$ T_H1 cells cause intestinal immunopathology via IFN-γ dependent Paneth cell death in conjunction with uncontrolled expansion of Gram-negative bacteria of the *Enterobacteriaceae* family.

Results

T. gondii infection triggers intestinal dysbiosis

Infection with *T. gondii* results in severe intestinal inflammation that is associated with qualitative shifts in the composition of the intestinal microbiota[18,19]. Quantitative analysis of intestinal bacteria revealed transient expansion of Proteobacteria that peaked 7 days post *T. gondii* infection, with the simultaneous loss of Bacteroidetes, while the relative abundance of Firmicutes remained largely unchanged (Fig. 1a, b and Supplementary Fig. 1). The observed dysbiosis was transient and resolved at the end of the acute responses to the parasite (Fig. 1a and Supplementary Fig. 1a–c). 454 pyrosequencing of the intestinal bacteria of infected mice also confirmed the dominance of Proteobacteria that appeared to be *Enterobacteriaceae*, a large family of Gram-negative bacteria frequently associated with intestinal inflammation and dysbiosis (Fig. 1c and Supplementary Fig. 2)[20,21]. Culture-based, 16S rRNA gene pyrosequencing, and *in situ* hybridization techniques demonstrated the expansion of Enterobacteriaceae and especially Escherichia spp. and Shigella spp. caused by T. gondii infection (Fig. 1c–f and Supplementary Fig. 2–3). Co-housing of *T. gondii*-infected mice with non-infected animals revealed that dysbiosis was restricted to infected mice and was not transmissible to non-infected littermate controls (Supplementary Fig. 4). This indicates that the presence of the parasite is essential for the selective expansion of *Enterobacteriaceae* (*Escherichia* spp. and *Shigella* spp.), because the parasite itself is not transmittable by fecal-oral transmission from infected to non-infected mice. These results

show that infection with *T. gondii* results in a quantitative shift in microbiota characterized by Proteobacteria dominance in the lumen of the inflamed intestine.

T. gondii infection triggers Paneth cell loss

Intestinal bacteria are controlled by antimicrobial peptides produced by Paneth cells and enterocytes[22,23]. To test if *T. gondii* triggers dysbiosis via aberrant induction of antimicrobial peptides (AMPs), we analyzed a panel of AMPs produced in naïve and infected mice. We observed a dramatic loss of lysozyme and defensin expression in the intestines of *T. gondii*-infected mice (Fig. 2a). This result was somewhat unexpected, because TLR ligands were shown to elicit induction of β-defensins and the bactericidal C-type lectin RegIII-γ [24–26], and the protozoan parasite *T. gondii* triggers potent TLR-dependent immune responses[5,17]. Parasitic infection resulted in the selective loss of Paneth cell-specific AMPs, as expression of RegIII-γ produced by multiple epithelial cell lineages[25] was unimpaired (Fig. 2b).

To investigate the loss of AMP expression in *T. gondii*-infected mice, we isolated small intestines from mice and analyzed Paneth cells in naïve and infected mice. We observed that the acute response to the parasite resulted in the disappearance of Paneth cells, which were practically undetectable by day 7 post-infection (Fig. 2c). Loss of Paneth cells was confirmed by electron microscopy experiments (Fig. 2d), suggesting that reduced expression of Paneth cell-specific AMPs was due to the disappearance of these cells. The disappearance of the Paneth cells was transient, with kinetics that closely recapitulated the dysbiosis observed in *T. gondii*-infected mice (Supplementary Fig. 5). Electron microscopy analysis of the Paneth cells revealed that the death of these cells was not the result of apoptosis, but was associated with mitochondrial damage in these cells (Supplementary Fig. 6). The ultrastructural analysis of dying Paneth cells during *T. gondii* infection also ruled out necrosis as a mechanism of Paneth cell elimination (Supplementary Fig. 6). Morphologically necrotic cells show a decrease in cell electron density and complete degradation of organelles and membranes not seen in Paneth cells during the course of *T. gondii* infection (Supplementary Fig. 6). Instead, at least some death of Paneth cells may be executed through necroptosis or a related mechanism of cell death associated with impaired mitochondrial functions[27]. These results suggest that the reduction in AMPs triggered by *T. gondii* infection was due to the physical loss of Paneth cells.

Microbiota is required for the *T. gondii*-mediated intestinal pathology

To examine the significance of the parasite induced dysbiosis we investigated if mice lacking intestinal bacteria develop intestinal damage when infected with *T. gondii*. We used germ-free mice that are microbiologically sterile and lack the intestinal microbiota, while germ-free mice colonized with a normal intestinal bacterial flora (conventionalized germ-free mice) were used as controls. In contrast to conventional and conventionalized mice (data not shown), *T. gondii*-infected germ-free mice did not develop intestinal pathology (Fig. 3a) and their Paneth cells were intact (Fig. 3b), suggesting that intestinal bacteria contribute to the development of intestinal inflammation.

To specifically address if *T. gondii* triggered dysbiosis characterized by expansion of Proteobacteria (*Enterobacteriaceae*) plays a role in intestinal pathology and Paneth cell death, we isolated *Enterobacteriaceae* (*E. coli*) from *T. gondii*-infected mice using *E. coli*-selective CHROMagar bacterial plates (Supplementary Fig. 3a) and adoptively transferred the bacteria into germ-free mice, alone or in combination with *T. gondii*. As controls, naïve and *T. gondii* infected germ-free mice were colonized with *Bacteroides fragilis*, a prominent intestinal *Bacteroides* species in mice. *Enterobacteriaceae* isolates resulted in intestinal pathology in the presence of *T. gondii* parasitic infection, whereas *B. fragilis* did not induce pathology in either condition (Fig. 3a). The observed intestinal pathology was associated with loss of Paneth cells (Fig. 3b). These results revealed that *T. gondii*-induced dysbiosis characterized by expansion of *Enterobacteriaceae* contributes to intestinal pathology and loss of Paneth cells.

T. gondii-induced Paneth cell loss is mediated by TLR11

Because TLR11 has a major role in initial parasite sensing via the detection of *T. gondii* profilin and induction of intestinal pathology during mucosal immune responses to the pathogen[17,28,29], we investigated if TLR11 and its downstream adaptor protein, MyD88, contribute to the loss of Paneth cells caused by toxoplasmosis. In contrast to wild-type mice, we observed minimal loss of Paneth cells in *Tlr11*$^{-/-}$ or *Myd88*$^{-/-}$ mice infected with *T. gondii* (Fig. 2 and Fig. 4a). Histological analysis of *Myd88*$^{-/-}$ mice revealed that Paneth cells were present at the base of each crypt, whereas some loss of Paneth cells was observed in *Tlr11*$^{-/-}$ mice infected with the parasite (Fig. 4a). Quantitative analysis of AMP expression showed minor (2- to 3-fold) loss of Paneth cell-specific proteins in TLR11- or MyD88- deficient mice (Fig. 4b), compared to undetectable (greater than 100-fold reduction) Paneth cell-specific AMPs in wild-type mice (Fig. 2a). In addition, quantification of *Proteobacteria* and *Bacteroidetes* revealed normal distribution of these taxa in infected *Myd88*$^{-/-}$ and *Tlr11*$^{-/-}$ mice (Fig. 4c). These results demonstrate that activation of TLR11 and MyD88 is required for the loss of Paneth cells triggered by the parasitic infection.

IFN-γ contributes to Paneth cell loss and intestinal dysbiosis

A major downstream effect of TLR-dependent recognition of pathogens is the induction of IFN-γ[2], which is required for host protection against parasites, but can also lead to severe immunopathology. Because TLR11 and MyD88 are major regulators of IFN-γ production in *T. gondii* infections[6,7,17], we next assessed whether the TLR11- and MyD88-mediated loss of Paneth cells was dependent on IFN-γ. Anti-IFN-γ, but not an isotype control antibody, completely prevented the loss of Paneth cells in *T. gondii*-infected mice (Fig. 5a). Furthermore, Paneth cells were intact in IFN-γ-deficient mice infected with *T. gondii*, despite dramatically elevated parasite loads detected in the intestines of these mice (Supplementary Fig. 7), suggesting IFN-γ was required for Paneth cell-loss.

Because Paneth cells were also intact in *T. gondii*-infected *Rag2*$^{-/-}$ mice (data not shown), we focused on CD4^{+} and CD8^{+} T cells as cellular sources of IFN-γ. Depletion of CD4^{+} T cells in wild-type mice largely prevented the loss of Paneth cells triggered by *T. gondii* infection (Fig. 5a). Quantitative analysis of AMPs in the intestines of mice infected with the parasite and treated with antibodies against IFN-γ or CD4 showed that elimination of Paneth

cells was dependent on IFN-γ and $CD4^+$ T cells (Fig. 5b). Depletion of $CD8^+$ T cells reduced Paneth cell loss, though with a lower impact than for $CD4^+$ antibody-mediated depletion (Fig. 5a, b). Wild-type $CD4^+$ T cells adoptively transferred into *Rag1*$^{-/-}$ or *Ifng*$^{-/-}$ hosts infected with *T. gondii* induced the elimination of Paneth cells (Supplementary Fig. 8), while adoptively-transferred $CD8^+$ T cells played a minor role in *T. gondii* triggered loss of Paneth cells (Supplementary Fig. 8). Finally, IFN-γ blockade in *Tlr11*$^{-/-}$ and *Myd88*$^{-/-}$ mice completely prevented the loss of AMPs triggered by *T. gondii* (data not shown). Thus, IFN-γ regulated by TLR11 and MyD88 was predominantly, even though incompletely, responsible for the parasite-induced loss of Paneth cells.

MyD88 signaling in T cells regulates an IFN-γ response

We next addressed the mechanisms by which $CD4^+$ T cells contribute to the IFN-γ- and TLR11- MyD88-dependent disappearance of Paneth cells. Despite a well-established role for dendritic cells (DCs) in the activation of T cells, mice with a DC-specific MyD88-deficiency have only minor defects in establishing systemic T_H1 immunity against *T. gondii*[16]. Similarly, mice with a DC-specific MyD88-deficiency (CD11c-Cre MyD88$^{fl/fl}$ mice) exhibited only a minor reduction in the frequency and absolute numbers of IFN-γ-secreting $CD4^+$ T cells during mucosal responses to *T. gondii* (Fig. 6a–c). MyD88 signaling in macrophages (as assessed in Mlys-Cre MyD88 $^{fl/fl}$ mice) and epithelial cells (in Villin-Cre MyD88 $^{fl/fl}$ mice) was also dispensable for the induction of IFN-γ-secreting $CD4^+$ T cells during mucosal responses to *T. gondii* (Fig. 6a–c). Simultaneous inactivation of MyD88 in DCs and macrophages in CD11c-Cre x Mlys-Cre MyD88$^{fl/fl}$ mice or in DCs and epithelial cells in CD11c-Cre x Villin-Cre MyD88$^{fl/fl}$ mice still resulted in induction of a high frequency and high absolute numbers of IFN-γ-producing $CD4^+$ T cells following *T. gondii* infection (Fig. 6). Furthermore, mice lacking MyD88 in DCs, macrophages or epithelial cells also lost Paneth cells during experimental toxoplasmosis (Fig. 7a, b and data not shown), indicating that MyD88 signaling in other cell type(s) apart from DCs, macrophages and epithelial cells induces T_H1 immunity and intestinal pathology.

Targeted inactivation of MyD88 in T cells in Lck-Cre MyD88$^{fl/fl}$ mice resulted in a reduction of IFN-γ-producing $CD4^+$ T cells that almost reproduced the one observed in *MyD88*$^{-/-}$ animals (Fig. 6). Furthermore, the Paneth cells were largely intact in *T. gondii*-infected Lck-Cre MyD88$^{fl/fl}$ mice (Fig. 7a,b) and these mice did not demonstrate the significant dysbiosis or intestinal pathology seen in the other MyD88-deficient mice analyzed (Fig. 7c and data not shown). However, quantitative analysis of T_H1 cells and microbiota showed Lck-Cre MyD88 $^{fl/fl}$ mice were not identical to *MyD88*$^{-/-}$ mice following *T. gondii* infection (Fig. 6b,c and Fig. 7c). Mice lacking MyD88 in both DCs and T cells (CD11c-Cre x Lck-Cre MyD88$^{fl/fl}$) had similar frequency and absolute numbers of T_H1 cells compared to *Myd88*$^{-/-}$ animals (Fig. 6b,c). We also observed that IL-1R-deficient mice, similar to *Casp1*$^{-/-}$ mice[28], exhibited normal T_H1 immunity to *T. gondii* (data not shown). Thus, we speculate that T cell-intrinsic TLR signaling or additional TLR and IL-1R independent T-cell intrinsic functions of MyD88 regulate IFN-γ secretion by $CD4^+$ T cells. In addition, T-cell intrinsic MyD88 signaling is linked to IFN-γ stability in T cells[30,31]. Taken together, these results revealed that the MyD88-signaling pathways in T cells is required for the induction of T_H1 responses against the parasite and subsequent intestinal

dysbiosis, where DC MyD88 plays a supplemental role in triggering IFN-γ production by $CD4^+$ T cells.

Discussion

Using a comprehensive panel of cell type-specific MyD88-deficient mice we demonstrate that T cell-intrinsic MyD88 signaling, rather than MyD88 activation in antigen-presenting cells, played a major role in T_H1 polarization during *T. gondii* infection. T cell-specific elimination of MyD88 reduced IFN-γ secretion by $CD4^+$ T cells. Moreover, *T. gondii*-infected T cell-specific MyD88-deficient mice, similar to complete MyD88-deficient animals, did not develop the IFN-γ and $CD4^+$ T cell-mediated dysbiosis responsible for the intestinal pathology seen in orally infected wild-type mice. These results are in contrast to both DC-specific MyD88-deficient mice and mice simultaneously lacking MyD88 in DCs and macrophages which demonstrate a modest reduction in T_H1 cells when compared with wild-type controls. Furthermore, lack of MyD88 in DCs and macrophages had no effect on *T. gondii*-induced intestinal dysbiosis and immunopathology characterized, as revealed here, by death of Paneth cells. This further dismisses the role of TLR signaling in antigen-presenting cells for T_H1-mediated immunity and immunopathology.

Previous studies have established that *Myd88*$^{-/-}$ mice, which cannot signal through IL-1 family receptors and most TLRs[1], including TLR11[17], are acutely susceptible to *T. gondii* infection[7]. *Myd88*$^{-/-}$ mice fail to activate T cells and produce IFN-γ essential for host resistance to the parasite[7,15]. *In vitro* $CD4^+$ T cell polarization assays using transgenic naïve $CD4^+$ T cells reveal the superior ability of wild-type DC to drive T_H1 differentiation from the same precursor pool when compared with *Myd88*$^{-/-}$ DCs[15]. The combination of *in vivo* phenotypes of *Myd88*$^{-/-}$ mice, *in vitro* T_H1 polarization assays, and the essential role for DCs in antigen-presentation[32] lead to a concept that activation of TLRs and the downstream adaptor protein MyD88 in antigen-presenting cells, specifically in DCs, trigger T_H1 responses[2]. The proposed model of innate control of adaptive immunity implies that MyD88 activation in DCs is solely responsible for induction of IFN-γ production by $CD4^+$ T cells. A major limitation of this concept is the lack of *in vivo* evidence since the conditional Myd88-deficient mice were unavailable. Instead, the phenotypes of *Myd88*$^{-/-}$ mice were extrapolated to TLR defects in innate immune cells[7]. Recent generation of *Myd88*$^{fl/fl}$ mice[33] allowed investigation of cell-type specific MyD88 functions involved in host defense against microbial pathogens.

Our recent analysis of DC-specific MyD88-deficient mice systemically infected with *T. gondii* unexpectedly revealed that MyD88 signaling in DCs is dispensable for the engagement of T cell responses[16]. While both *Myd88*−/− and DC-specific MyD88-deficient mice are highly susceptible to the parasitic infection, activation of $CD4^+$ and $CD8^+$ T cells is impaired only in *Myd88*−/− mice and is largely intact in mice lacking MyD88 only in DCs. The examination of DC-specific MyD88-deficient mice uncovered that TLR activation in DCs promotes IFN-γ production by NK cells rather than T cells. MyD88 signaling in DCs is required for early IFN-γ production by NK cells which is critical for limiting the infection until T cells can contribute to immune control of the parasite[16]. These results strongly implicate a major defect in the innate immune response as being responsible for the acute

susceptibility of DC-specific MyD88-deficient mice to *T. gondii* infection[16], but left unanswered a fundamental question regarding cell-type specific requirements for MyD88 in the regulation of T_H1 immunity. This question is of particular relevance for mucosal responses to *T. gondii*. In addition to leukocytes, mucosal epithelial cells are involved in TLR-mediated sensing of both the parasite and commensal bacteria[28]. Specifically it is the intestinal microbiota that potentiates IFN-γ production by $CD4^+$ T cells in response to *T. gondii* infection[28]. It appears that TLR11-mediated parasite recognition cooperates with the TLR4 and TLR9-dependent effects of intestinal bacteria on the outcome of the IFN-γ production and intestinal pathology[28], but the cellular biology of TLR-dependent MyD88 activation responsible for T_H1 mediated immunity and immunopathology is not known. These further emphasize the importance of understanding mechanisms regulating IFN-γ production by $CD4^+$ T cells in response to TLR-mediated activation Our current *in vivo* experiments formally established a T cell-intrinsic MyD88 signaling pathway in regulation of T_H1 effector choice. Furthermore, our results also ruled out a role for MyD88 in epithelial cells, macrophages, and B cells, in addition to DCs, for controlling IFN-γ production by $CD4^+$ T cells. These observations indicate that we have just begun to understand to what extent MyD88 signaling in cells of both innate and adaptive immunity contributed to host defense. MyD88 in epithelial cells regulates their proliferation and expression of AMPs[24,26,34–36]; B cell-intrinsic MyD88 is involved in augmenting IgM secretion[37] and in T cell -dependent antibody production in response to viral particles[38]; as established in this work, T cell-intrinsic MyD88 regulated T_H1 polarization. Altogether, these experiments suggest remarkable cell-type specific MyD88 functions where further work is needed to identify the relevant MyD88 activators in different cell types.

In addition to identification of MyD88 in T cells as a central molecule regulating IFN-γ by $CD4^+$ T cells, our experiments reveal a mechanism responsible for severe intestinal inflammation mediated by T_H1 cells. We show that IFN-γ production primarily by $CD4^+$ T cells during *T. gondii* infection resulted in the death of Paneth cells, loss of their AMPs and the subsequent expansion of intestinal bacteria, the majority of which appeared to be *Enterobacteriaceae*. These results add to a growing body of literature indicating that IFN-γ, as an essential host protection factor, is also responsible for host tissue damage[39,40]. We also established that *T. gondii* infection in germ-free mice, in the absence of intestinal bacteria, was not sufficient for intestinal inflammation and the loss of Paneth cells. Instead, the pathogen-induced intestinal dysbiosis, and in particular the presence of *Proteobacteria*, were crucial for the development of intestinal inflammation and the IFN-γ-dependent death of Paneth cells during parasitic infection. These results are in agreement with the ability of intestinal bacteria to potentiate a T_H1 response to the parasite[28] that, while required for host protection, is also involved in intestinal pathology characterized by Paneth cell death. Overall, our investigation of cell type-specific factors regulating T_H1 polarization during *T. gondii* infection identified a T cell-intrinsic MyD88 pathway as a major regulator of IFN-γ production in $CD4^+$ T cells responsible for lethal intestinal pathology triggered by the parasite.

Methods

Animals

C57BL/6 mice were obtained from the University of Texas Southwestern (UTSW) Medical Center Mouse Breeding Core Facility. RAG2$^{-/-}$ and IFN-γ$^{-/-}$ mice were obtained from Jackson Laboratory. *Tlr11*$^{-/-}$ and *Myd88*$^{-/-}$ mice have been previously described in experimental toxoplasmosis studies[41,42]. *Myd88*^{flox} (B6.129P2-*Myd88*^{tm1Defr}), *Myd88*$^{flox/flox}$ × CD11c-Cre (DC-*Myd88*$^{-/-}$), *Myd88*$^{flox/flox}$ × Villin-Cre (E-*Myd88*$^{-/-}$), *Myd88*$^{flox/flox}$ × CD19-Cre (B-*Myd88*$^{-/-}$), *Myd88*$^{flox/flox}$ × Lck-Cre (T-*Myd88*$^{-/-}$), and *Myd88*$^{flox/flox}$ × LysM-Cre (M-*Myd88*$^{-/-}$) mice have been described previously[43]. In this study, the *Myd88*^{flox} mice were additionally crossed to CD11c-Cre × Lck-Cre and LysM-Cre × CD11c-Cre deleter mice. RegIII-γ$^{-/-}$ mice were previously described[44].

Control and experimental mice were age-matched within individual experiments. All mice were maintained at the American Association of Laboratory Animal Care-accredited animal facility at the UTSW Medical Center. All of the animals that were used were age- and sex-matched. All mice were maintained in the same animal room.

Toxoplasma gondii infections, histopathology, and RT-PCR

All mice were infected orally with an average of 20 *T. gondii* cysts (ME49 strain). At days 3, 5, 7, 10 and 14 post-infection, the animals were necropsied, and portions of the small intestines were fixed in Carnoy's fixative, embedded in paraffin, sectioned at 5 μm, and stained with hematoxylin and eosin or Alcian blue or used for in situ hybridization. For in situ hybridization, after deparaffinization and rehydration in hybridization buffer (0.9 M NaCl, 0.1% SDS and 20 mM Tris-HCl, pH 7.4), the small intestines were incubated overnight at 50°C in the dark with Alexa-488-conjugated *Enterobacteriaceae*-specific ENTBAC (5′-catgaatcacaaagtggtaagcgcc-3′) and Alexa-532-conjugated eubacteria EUB338 (5′-gctgcctcccgtaggagt-3′) probes for bacterial 16S rRNA genes[45]. The probes were diluted to final concentrations of 1 ng/μl in hybridization solution. The sections were then washed three times with a hybridization solution for 15 minutes, counterstained with SYTO62, and mounted using ProLong Gold Antifade Reagent (Invitrogen). The sections were imaged using a Leica SPE system fitted with a Leica 63X objective NA 1.4. The datasets were processed using Leica Advanced Fluorescence software (Leica).

For electron microscopy analysis, the small intestines were fixed in 2.5% glutaraldehyde in 0.1 M sodium cacodylate, followed by 1% osmium tetroxide in 0.1 M sodium cacodylate. The samples were embedded in epoxy resin (Electron Microscopy Sciences) and polymerized at 60°C. Ultrathin sections were cut at 80 nm and stained with uranyl acetate and lead citrate. Sections were examined at 120 KV with a Tecnai G2 Spirit transmission electron microscope (FEI Company), and the images were recorded on a Gatan USC1000 2k CCD camera (Gatan).

Total RNA was isolated from the intestines of naïve or *T. gondii*-infected mice using Trizol with subsequent purification using a PureLink RNA Mini Kit (Invitrogen). cDNA was prepared using a SuperScript III Kit (Invitrogen). Optimized primers targeting each gene were designed using Primer 3 software[46]. These primers included the following: Lyz1, 5′-

gccaaggtctacaatcgttgtgagttg-3′, 5′-cagtcagccagcttgacaccacg-3′; Alpha-defensin 1, also known as Defcr1, 5′-tcaagaggctgcaaaggaagagaac-3′, 5′-tggtctccatgttcagcgacagc-3′; Defensin, alpha, 21 (Defa21, also known as Defcr21), 5′-ccaggggaagatgaccaggctg-3′, 5′-tgcagcgacgatttctacaaaggc- 3′; Defa-rs1, defensin alpha-related sequence 1, 5′-caccacccaagctccaaatacacag-3′, 5′-atcgtgaggaccaaaagcaaatgg-3′, Cryptdin 2, CR2, 5′-ccaggctgatcctatccaaa-3′, 5′-gtcccattcatgcgttctct-3′; Reg3-γ, 5′-aacagaggtggatgggagtg-3′, 5′-ggccttgaatttgcagacat-3′; and Hprt, 5′-gcccttgactataatgagtacttcagg-3′, 5′-ttcaacttgcgctcatcttagg-3′[46]. cDNA was amplified using SsoFast Eva Green Supermix (BioRad). A MyiQ Real-Time PCR Detection System (BioRad) was used to obtain Ct values. The relative expression of each sample was determined after normalization to HPRT using the ddCt method.

Bacterial cultures and sequencing

To detect anaerobic and aerobic bacterial colonies in the lumen of the small intestine, the luminal contents were harvested from naïve and *T. gondii*-infected mice. Aerobic bacteria were grown on blood and CHROMagar plates. Anaerobic bacteria were grown on blood agar using an anaerobic vented jar (BD Biosciences)[41]. Culturable bacteria counts were obtained by plating serial dilutions of bacteria on the corresponding media. Bacterial genomic DNA was extracted from the small intestinal luminal content on days 3, 5, 7, 10 and 14 post-infection using a Qiagen DNeasy Kit according to the manufacturer's instructions. Broad-range 16S rDNA PCR (forward primer, 5′-agagtttgatymtggctcag-3′ and reverse primer, 5′-acggytaccttgttacgactt-3′) was used to amplify and clone the bacterial DNA present in the individual samples without any prior cultivation. The cloned inserts were identified through sequencing of the 16S rDNA gene fragments using the pCR2.1 vector-specific M13 reverse and T7 promoter primers. The DNA sequences were interpreted by comparing the retrieved sequences with those stored in the GenBank database using the basic local alignment software tool (BLAST; National Center for Biotechnology Information) and the Seqmatch tool (Ribosomal Database Project).

For 454-based DNA pyrosequencing, genomic DNA isolated using a DNA stool kit (QIAGEN) was further purified using a DNA clean-up kit (MoBio). Bacterial Tag-Encoded FLX 454-Pyroseqencing was carried out using barcoded primers 28F-519R for the V1–V3 region of the 16S rRNA gene by the Research and Testing Laboratory (Lubbock, TX).

Relative and absolute quantification of intestinal bacteria by qPCR

The relative abundances of Bacteroidetes, Firmicutes, and Proteobacteria (family *Enterobacteriaceae*) were measured by qPCR using a MyiQ Real-Time PCR Detection System with taxon-specific or universal 16S rRNA gene primers. The primers used were as follows: Firmicutes, 928F-Firm, 5′-tgaaactyaaaggaattgacg-3′ and 1040FirmR, 5′-accatgcaccacctgtc-3′[47] or Firm934F, 5′-ggagyatgtggtttaattcgaagca-3′ and Firm1060R, 5′-agctgacgacaaccatgcac-3′[48]; Bacteroidetes, 798cfbF, 5′-craacaggattagataccct-3′, and cfb967R, 5′-ggtaaggttcctcgcgtat-3′[48] or BactF285, 5′-ggttctgagaggaggtccc-3′, and UniR338, 5′-gctgcctcccgtaggagt-3′[49]; γ-Proteobacteria, 1080gF, 5′-tcgtcagctcgtgtygtga-3′, and g1202R, 5′-cgtaagggccatgatg-3′[47]; and *Enterobacteriaceae*, Uni515F, 5′-gtgccagcmgccgcggtaa-3′, and Ent826R, 5′-gcctcaagggcacaacctccaag-3′[50].

To complement the relative qPCR approach developed initially, a plasmid-based method for quantification of intestinal dysbiosis was utilized. Specifically, absolute bacterial abundance was determined using standard curves produced from serial dilutions of cloned bacterial DNA corresponding to a short segment of the 16S rRNA gene that was amplified using conserved 16S rRNA gene specific primers as described previously[44]. Briefly, the abundance of *Proteobacteria*, *Bacteroidetes*, *and Firmicutes* were determined by the use of taxon-specific 16S rRNA gene primers that were also used for relative abundance determination (*Proteobacteria*, forward primer 5′-gtgccagcmgccgcggtaa-3′ and reverse primer 5′-gcctcaagggcacaacctccaag-3′; *Bacteroidetes*, forward primer 5′-ggttctgagaggaggtccc-3′ and reverse primer 5′-gctgcctcccgtaggagt-3′; *Firmicutes*, forward primer 5′-ggagyatgtggtttaattcgaagca-3′ and reverse primer 5′-agctgacgacaaccatgcac-3′). Threshold cycle (C_t) was plotted against plasmid copy number to produce each standard curve; GraphPad Prism analysis of each semilog line by nonlinear regression produced an equation relating C_t value to 16S rRNA gene copy number. C_t values of the samples were converted to copy number using this equation and reported as 16S rRNA copies. The 16S rRNA copies per lumen were calculated by multiplying by the amount of DNA present in the sample. It should be noted that this qPCR method measures 16S rRNA gene copies per sample, not actual bacterial numbers or colony forming units. Percentage of taxa in the small intestine was determined by dividing the taxon-specific 16S rRNA gene copy number by the eubacteria (universal) 16S rRNA gene copy number.

Ex Vivo Measurement of CD4$^+$ T-Cell Responses

To assay the responses of mice infected with *T. gondii*, the mesenteric lymph nodes were harvested from WT, *Myd88*$^{-/-}$, and cell type-specific MyD88-deficient mice on day 7 post-infection. Single cell suspensions were restimulated with 1 μg/ml αCD3 (BD Biosciences) for 5 hr in the presence of GolgiPlug (Brefeldin A, BD Biosciences). After in vitro restimulation, the cells were washed once in PBS + 1% FBS and stained with fluorochrome-conjugated antibodies. Cell fluorescence was measuredusing a FACSCalibur or LSRII flow cytometer, and data were analyzed using FlowJo software (Tree Star).

To quantify the deletion efficiency of MyD88 in T cells in the T-*Myd88*$^{-/-}$ mice, genomic DNA was extracted from sort-purified T cells. The residual amount of the “floxed” region was quantified by Taqman PCR using primers (Forward 5′-gttgtgtgtgtccgaccgtg-3′, reverse 5′-tctcaattagctcgctggca-3′) and a Taqman probe 5′-FAM-tgccgggcacctgtgtctgg-Blackhole-3′ on an ABI PRISM 7300 sequence detection system as described previously[51]. Depletion of MyD88 in T cells achieved by Lck-cre deleter was at least 96%. The genomic DNA from Lck-cre negative Myd88$^{fl/fl}$ mice was used for the no-deletion control.

Statistical analysis

All data were analyzed with Prism (Version 5; GraphPad). Data were considered statistically significant for P values less than 0.05 using a two-tailed t-test.

Supplementary Material

Refer to Web version on PubMed Central for supplementary material.

Acknowledgments

This research was supported by NIH R01 AI085263 to F.Y, NIH R01 DK070855 to L.V.H., and the Howard Hughes Medical Institute (L.V.H.). C.R.S. was supported in part by NIH A1005284-33. We would also like to thank Cassie Behrendt and Charmaine Clements for germ- free mouse husbandry.

References

1. Kawai T, Akira S. Toll-like receptors and their crosstalk with other innate receptors in infection and immunity. Immunity. 2011; 34:637–650. [PubMed: 21616434]
2. Iwasaki A, Medzhitov R. Regulation of adaptive immunity by the innate immune system. Science. 2010; 327:291–295. [PubMed: 20075244]
3. Beutler B. Microbe sensing, positive feedback loops, and the pathogenesis of inflammatory diseases. Immunol Rev. 2009; 227:248–263. [PubMed: 19120489]
4. Medzhitov R, Schneider DS, Soares MP. Disease tolerance as a defense strategy. Science. 2012; 335:936–941. [PubMed: 22363001]
5. Gazzinelli RT, Denkers EY. Protozoan encounters with Toll-like receptor signalling pathways: implications for host parasitism. Nat Rev Immunol. 2006; 6:895–906. [PubMed: 17110955]
6. Sukhumavasi W, et al. TLR adaptor MyD88 is essential for pathogen control during oral toxoplasma gondii infection but not adaptive immunity induced by a vaccine strain of the parasite. J Immunol. 2008; 181:3464–3473. [PubMed: 18714019]
7. Scanga CA, et al. Cutting edge: MyD88 is required for resistance to Toxoplasma gondii infection and regulates parasite-induced IL-12 production by dendritic cells. J Immunol. 2002; 168:5997–6001. [PubMed: 12055206]
8. Scharton-Kersten TM, et al. In the absence of endogenous IFN-gamma, mice develop unimpaired IL-12 responses to Toxoplasma gondii while failing to control acute infection. J Immunol. 1996; 157:4045–4054. [PubMed: 8892638]
9. Lieberman LA, et al. IL-23 provides a limited mechanism of resistance to acute toxoplasmosis in the absence of IL-12. J Immunol. 2004; 173:1887–1893. [PubMed: 15265921]
10. Suzuki Y, Orellana MA, Schreiber RD, Remington JS. Interferon-gamma: the major mediator of resistance against Toxoplasma gondii. Science. 1988; 240:516–518. [PubMed: 3128869]
11. Gazzinelli RT, et al. In the absence of endogenous IL-10, mice acutely infected with Toxoplasma gondii succumb to a lethal immune response dependent on CD4+ T cells and accompanied by overproduction of IL-12, IFN-gamma and TNF-alpha. J Immunol. 1996; 157:798–805. [PubMed: 8752931]
12. Jankovic D, et al. Conventional T-bet(+)Foxp3(-) Th1 cells are the major source of host-protective regulatory IL-10 during intracellular protozoan infection. J Exp Med. 2007; 204:273–283. [PubMed: 17283209]
13. Jankovic D, Kugler DG, Sher A. IL-10 production by CD4+ effector T cells: a mechanism for self-regulation. Mucosal Immunol. 2010; 3:239–246. [PubMed: 20200511]
14. Egan CE, Cohen SB, Denkers EY. Insights into inflammatory bowel disease using Toxoplasma gondii as an infectious trigger. Immunol Cell Biol. 2011
15. Jankovic D, et al. In the absence of IL-12, CD4(+) T cell responses to intracellular pathogens fail to default to a Th2 pattern and are host protective in an IL-10(−/−) setting. Immunity. 2002; 16:429–439. [PubMed: 11911827]
16. Hou B, Benson A, Kuzmich L, DeFranco AL, Yarovinsky F. Critical coordination of innate immune defense against Toxoplasma gondii by dendritic cells responding via their Toll-like receptors. Proc Natl Acad Sci U S A. 2011; 108:278–283. [PubMed: 21173242]
17. Yarovinsky F, et al. TLR11 activation of dendritic cells by a protozoan profilin-like protein. Science. 2005; 308:1626–1629. [PubMed: 15860593]
18. Erridge C, Duncan SH, Bereswill S, Heimesaat MM. The induction of colitis and ileitis in mice is associated with marked increases in intestinal concentrations of stimulants of TLRs 2, 4, and 5. PLoS One. 2010; 5:e9125. [PubMed: 20161736]

19. Heimesaat MM, et al. Gram-negative bacteria aggravate murine small intestinal Th1-type immunopathology following oral infection with Toxoplasma gondii. J Immunol. 2006; 177:8785–8795. [PubMed: 17142781]
20. Garrett WS, et al. Enterobacteriaceae act in concert with the gut microbiota to induce spontaneous and maternally transmitted colitis. Cell Host Microbe. 2010; 8:292–300. [PubMed: 20833380]
21. Willing BP, et al. A pyrosequencing study in twins shows that gastrointestinal microbial profiles vary with inflammatory bowel disease phenotypes. Gastroenterology. 2010; 139:1844–1854. e1841. [PubMed: 20816835]
22. Bevins CL, Salzman NH. Paneth cells, antimicrobial peptides and maintenance of intestinal homeostasis. Nat Rev Microbiol. 2011; 9:356–368. [PubMed: 21423246]
23. Wehkamp J, Koslowski M, Wang G, Stange EF. Barrier dysfunction due to distinct defensin deficiencies in small intestinal and colonic Crohn's disease. Mucosal Immunol. 2008; 1 (Suppl 1):S67–74. [PubMed: 19079235]
24. Vora P, et al. Beta-defensin-2 expression is regulated by TLR signaling in intestinal epithelial cells. J Immunol. 2004; 173:5398–5405. [PubMed: 15494486]
25. Vaishnava S, Behrendt CL, Ismail AS, Eckmann L, Hooper LV. Paneth cells directly sense gut commensals and maintain homeostasis at the intestinal host-microbial interface. Proc Natl Acad Sci U S A. 2008; 105:20858–20863. [PubMed: 19075245]
26. Brandl K, Plitas G, Schnabl B, DeMatteo RP, Pamer EG. MyD88-mediated signals induce the bactericidal lectin RegIII gamma and protect mice against intestinal Listeria monocytogenes infection. J Exp Med. 2007; 204:1891–1900. [PubMed: 17635956]
27. Yuan J, Kroemer G. Alternative cell death mechanisms in development and beyond. Genes Dev. 2010; 24:2592–2602. [PubMed: 21123646]
28. Benson A, Pifer R, Behrendt CL, Hooper LV, Yarovinsky F. Gut commensal bacteria direct a protective immune response against Toxoplasma gondii. Cell Host Microbe. 2009; 6:187–196. [PubMed: 19683684]
29. Plattner F, et al. Toxoplasma profilin is essential for host cell invasion and TLR11-dependent induction of an interleukin-12 response. Cell Host Microbe. 2008; 3:77–87. [PubMed: 18312842]
30. Sun D, Ding A. MyD88-mediated stabilization of interferon-gamma-induced cytokine and chemokine mRNA. Nat Immunol. 2006; 7:375–381. [PubMed: 16491077]
31. Han J. MyD88 beyond Toll. Nat Immunol. 2006 Apr; 7(4):370–1. [PubMed: 16550203]
32. Mellman I, Steinman RM. Dendritic cells: specialized and regulated antigen processing machines. Cell. 2001; 106:255–258. [PubMed: 11509172]
33. Hou B, Reizis B, DeFranco AL. Toll-like receptors activate innate and adaptive immunity by using dendritic cell-intrinsic and -extrinsic mechanisms. Immunity. 2008; 29:272–282. [PubMed: 18656388]
34. Rakoff-Nahoum S, Paglino J, Eslami-Varzaneh F, Edberg S, Medzhitov R. Recognition of commensal microflora by toll-like receptors is required for intestinal homeostasis. Cell. 2004; 118:229–241. [PubMed: 15260992]
35. Vaishnava S, et al. The antibacterial lectin RegIIIgamma promotes the spatial segregation of microbiota and host in the intestine. Science. 2011; 334:255–258. [PubMed: 21998396]
36. Abreu MT. Toll-like receptor signalling in the intestinal epithelium: how bacterial recognition shapes intestinal function. Nat Rev Immunol. 2010; 10:131–144. [PubMed: 20098461]
37. Kirkland D, et al. B cell-intrinsic MyD88 signaling prevents the lethal dissemination of commensal bacteria during colonic damage. Immunity. 2012; 36:228–238. [PubMed: 22306056]
38. Hou B, et al. Selective utilization of Toll-like receptor and MyD88 signaling in B cells for enhancement of the antiviral germinal center response. Immunity. 2011; 34:375–384. [PubMed: 21353603]
39. Damsker JM, Hansen AM, Caspi RR. Th1 and Th17 cells: adversaries and collaborators. Ann N Y Acad Sci. 2010; 1183:211–221. [PubMed: 20146717]
40. Strober W, Fuss IJ. Proinflammatory cytokines in the pathogenesis of inflammatory bowel diseases. Gastroenterology. 2011; 140:1756–1767. Methods associated references. [PubMed: 21530742]

41. Benson A, Pifer R, Behrendt CL, Hooper LV, Yarovinsky F. Gut commensal bacteria direct a protective immune response against Toxoplasma gondii. Cell Host Microbe. Aug 20.2009 6:187. [PubMed: 19683684]
42. Yarovinsky F, et al. TLR11 activation of dendritic cells by a protozoan profilin-like protein. Science. Jun 10.2005 308:1626. [PubMed: 15860593]
43. Kirkland D, et al. B cell-intrinsic MyD88 signaling prevents the lethal dissemination of commensal bacteria during colonic damage. Immunity. Feb 24.2012 36:228. [PubMed: 22306056]
44. Vaishnava S, et al. The antibacterial lectin RegIIIgamma promotes the spatial segregation of microbiota and host in the intestine. Science. 2011; 334:255–258. [PubMed: 21998396]
45. Jansen GJ, et al. Rapid identification of bacteria in blood cultures by using fluorescently labeled oligonucleotide probes. J Clin Microbiol. Feb.2000 38:814. [PubMed: 10655390]
46. Rozen S, Skaletsky H. Primer3 on the WWW for general users and for biologist programmers. Methods Mol Biol. 2000; 132:365–386. [PubMed: 10547847]
47. Bacchetti De Gregoris T, Aldred N, Clare AS, Burgess JG. Improvement of phylum- and class-specific primers for real-time PCR quantification of bacterial taxa. J Microbiol Methods. 2011; 86:351–356. [PubMed: 21704084]
48. Guo X, et al. Development of a real-time PCR method for Firmicutes and Bacteroidetes in faeces and its application to quantify intestinal population of obese and lean pigs. Lett Appl Microbiol. 2008; 47:367–373. [PubMed: 19146523]
49. Dore J, Sghir A, Hannequart-Gramet G, Corthier G, Pochart P. Design and evaluation of a 16S rRNA-targeted oligonucleotide probe for specific detection and quantitation of human faecal Bacteroides populations. Syst Appl Microbiol. 1998; 21:65–71. [PubMed: 9741111]
50. Barman M, et al. Enteric salmonellosis disrupts the microbial ecology of the murine gastrointestinal tract. Infect Immun. 2008; 76:907–915. [PubMed: 18160481]
51. Hou B, Reizis B, DeFranco AL. Toll-like receptors activate innate and adaptive immunity by using dendritic cell-intrinsic and -extrinsic mechanisms. Immunity. 2008; 29:272–282. [PubMed: 18656388]

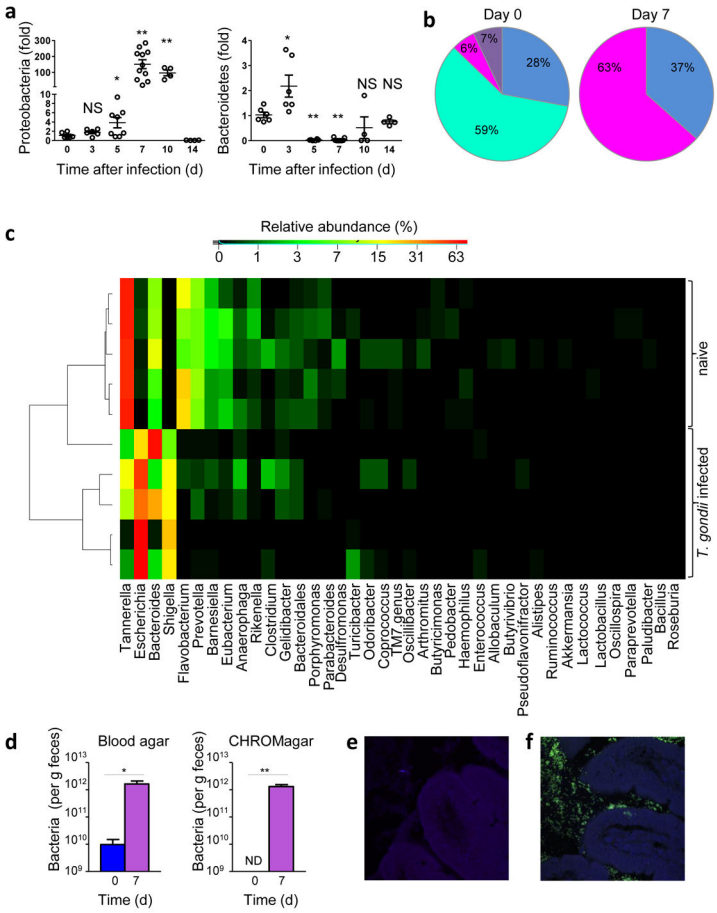

Figure 1. *T. gondii* infection results in intestinal dysbiosis

(**a**) qRT-PCR analysis of Proteobacteria and Bacteroidetes loads in the lumens of small intestines of wild-type mice left untreated (d0) or infected orally with 20 cysts of the *T. gondii* ME49 strain per mouse at the indicated time post-infection. The results are representative of four independent experiments, each involving at least five mice per group. * P< 0.05; ** P< 0.01. (**b**) Genomic DNA analysis of microbial communities from the lumens of naïve or *T. gondii*-infected wild-type mice on day 7 post-infection (n= 5–7 mice/group). For each mouse, 192 colonies containing cloned 16rRNA amplicons were processed for sequencing. The relative frequencies of Proteobacteria (magenta), Bacteroidetes (turquoise), Firmicutes (Blue), and other phyla (purple) are shown. Bacteroidetes were not detected in samples prepared from *T. gondii*-infected mice. (**c**) Heatmap of the relative abundance of the 40 most dominant genera in the small intestines of naïve or *T. gondii*-infected wild-type mice as determined by genomic DNA analysis by 454-based DNA pyrosequencing. Samples are sorted based on hierarchical clustering of weighted unifrac distances. (**d**) Bacterial loads in the lumens of the small intestines of non-infected (d0) or *T. gondii*-infected mice (d7) analyzed by plating bacteria on blood agar or CHROMagar plates under aerobic conditions. * P< 0.05; ** P< 0.001 (**e**) *In situ* hybridization of Proteobacteria (green) in non-infected or (**f**) *T. gondii*-infected mice. The results are representative of four independent experiments, each involving at least five mice per group.

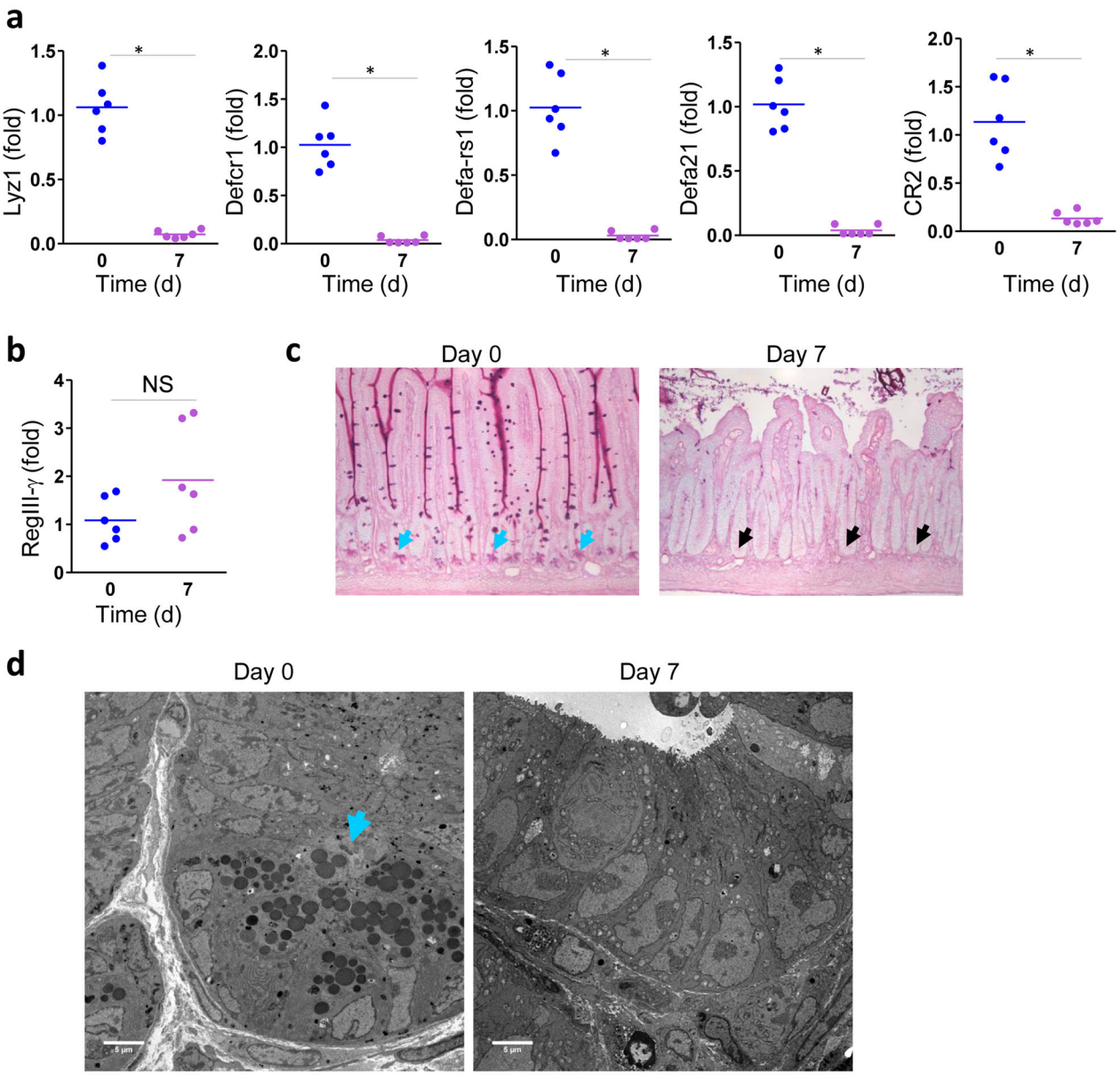

Figure 2. *T. gondii* infection results in loss of Paneth cells

(a) qRT-PCR analysis of Lyz1, Defcr1 (alpha-defensin-1), Defa-rs1, Defa21, and CR2 were measured in the small intestines of untreated mice (n=6, blue) or infected orally with 20 cysts per mouse of the ME49 on day 7 post-infection (n=6, purple). * P< 0.001 (**b**) qRT-PCR analysis of RegIII-γ in the small intestines of naïve (n=6) and infected (n=6) mice. (**c**) Histological visualization of Paneth cells in the small intestines of naïve and infected (d7) mice. The results are representative of four independent experiments, each involving at least six mice per group. The blue arrows indicate Paneth cells and the black arrows point toward bases of the crypts lacking these cells. (**d**) Electron microscopy analysis of the bases of the crypts in naïve and *T. gondii*-infected mice (3 mice per group). The blue arrows indicate Paneth cells. The results are representative of four independent experiments.

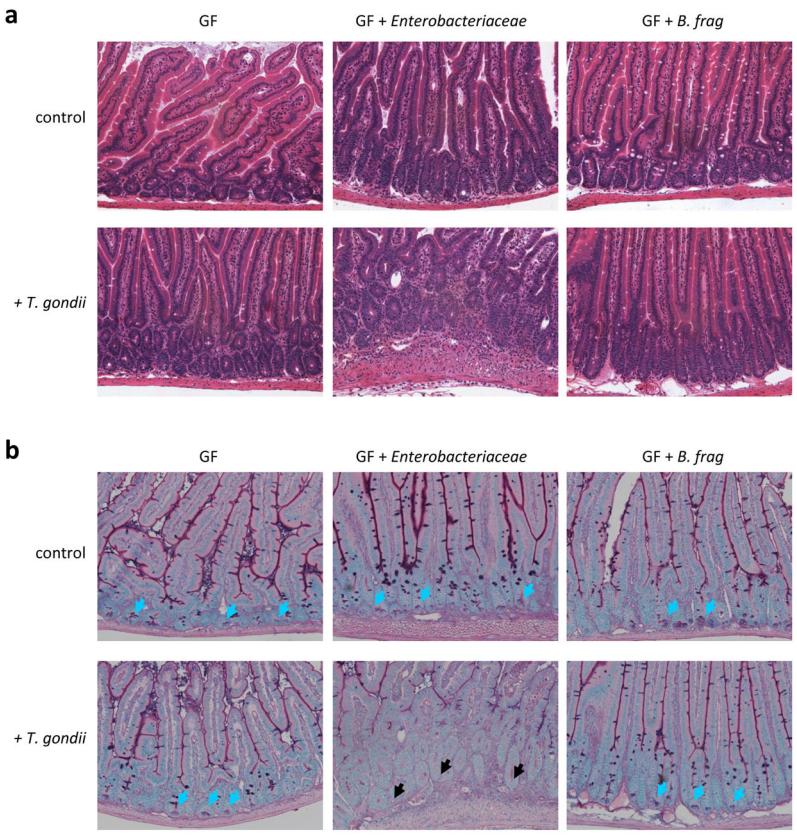

Figure 3. *T. gondii*-induced dysbiosis contributes to the intestinal pathology

(a) Germ-free (GF) mice were left untreated, colonized with the *Enterobactericeae* isolate (Supplemental Fig. 3a), or with *Bacteroides fragiles* (*B. frag*), and infected orally with 20 cysts of the *T. gondii* ME49 strain. Histological analysis of the small intestine was performed on day 7 post-infection. The results are representative of two independent experiments. **(b)** Germ-free (GF) mice were mock colonized, colonized with the *Enterobactericeae* isolate (Supplemental Fig. 3a), or with *B. frag*, and additionally infected orally with *T. gondii*. Histological visualization of Paneth cells in the small intestines were performed on day 7 post-infection. The blue arrows indicate Paneth cells and the black arrows point toward bases of the crypts lacking these cells. The results are representative of two independent experiments.

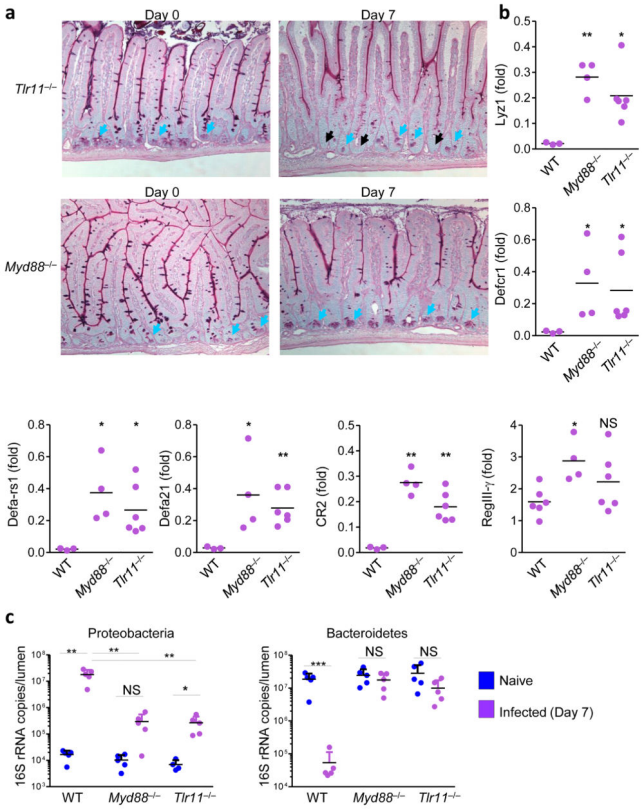

Figure 4. TLR11-mediated activation of MyD88 triggers Paneth cell death and intestinal dysbiosis

(**a**) WT (not shown), *Tlr11*$^{-/-}$, and *Myd88*$^{-/-}$ mice (five mice per group) were left untreated or were infected orally with 20 cysts per mouse of the ME49 strain of *T. gondii*. Histological visualization of Paneth cells in the small intestines were performed on day 7 post-infection. The blue arrows indicate Paneth cells and the black arrows point toward bases of the crypts lacking these cells. (**b**) The relative expression levels of Defcr1 (alpha-defensin-1), Defa-rs1, Defa21, CR2, and RegIII-γ were measured by qRT-PCR in the small intestines of WT (n=3), *Tlr11*$^{-/-}$ (n=6), and *Myd88*$^{-/-}$ (n=4) mice on day 7 post-infection. * P< 0.05; ** P< 0.01. (**c**) qRT-PCR analysis of Proteobacteria and Bacteroidetes in the lumens of small intestines of naïve (blue) or *T. gondii*-infected (purple) mice. The data shown are the means ± SD. * P< 0.05; ** P< 0.01; *** P< 0.001. The results are representative of >10 independent experiments, each involving 3–7 mice per group.

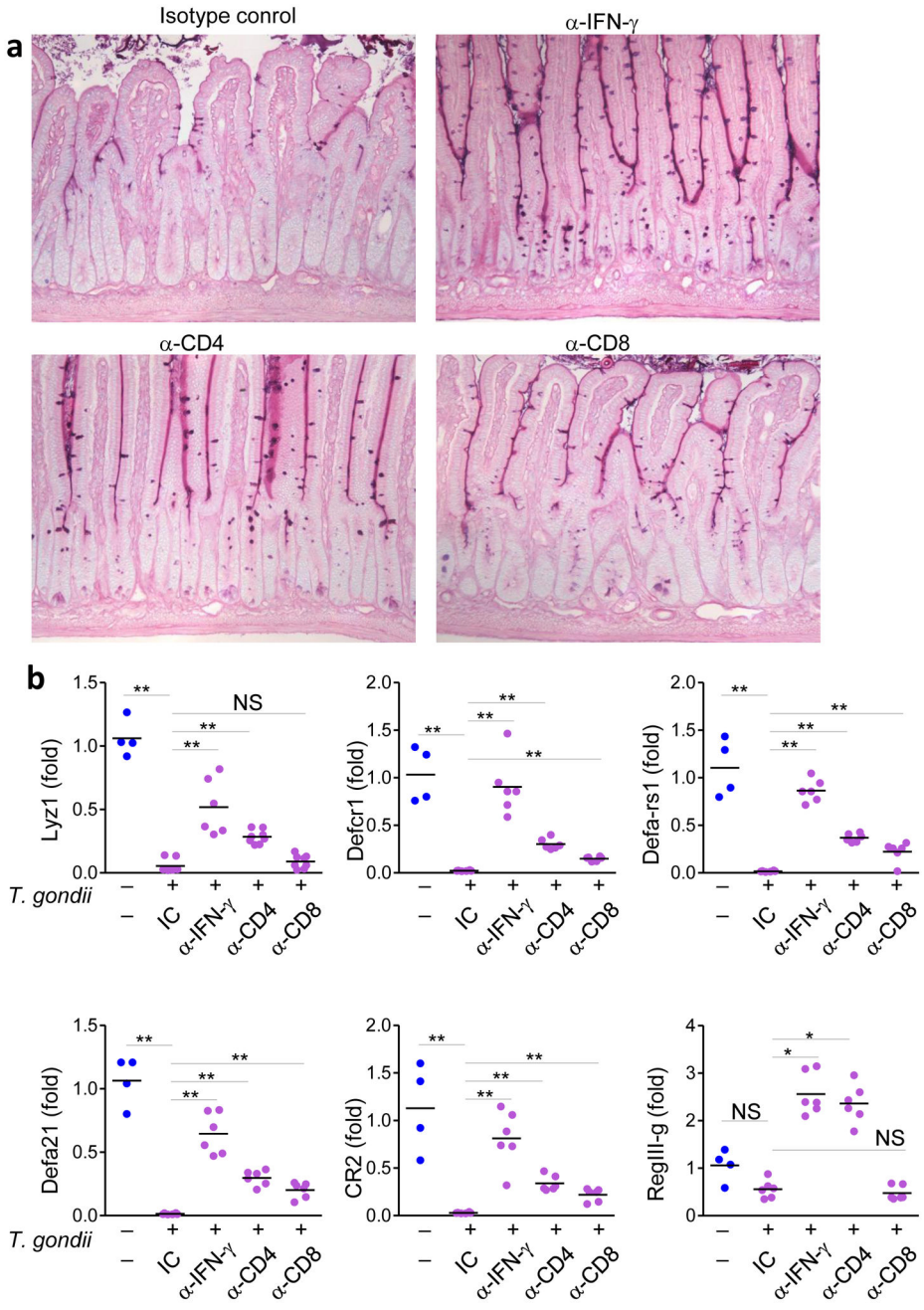

Figure 5. IFN-γ mediates loss of Paneth cells

(**a**) WT mice were treated with isotype control (IC), α-IFN-γ, α-CD4, or α-CD8 antibodies and then infected orally with 20 cysts per mouse of the ME49 strain of *T. gondii*. Histological analyses of Paneth cells in small intestines were performed on day 7 post-infection. (**b**) qRT-PCR analysis of Lyz1, Defcr1 (alpha-defensin-1), Defa-rs1, Defa21, CR2, and RegIII-γ were measured in the small intestines of naïve (blue) or *T. gondii*-infected WT mice treated with IC, α-IFN-γ, α-CD4, or α-CD8 antibodies (purple). * P< 0.05; ** P< 0.01. The results are representative of three independent experiments, each involving 4–7 mice per group.

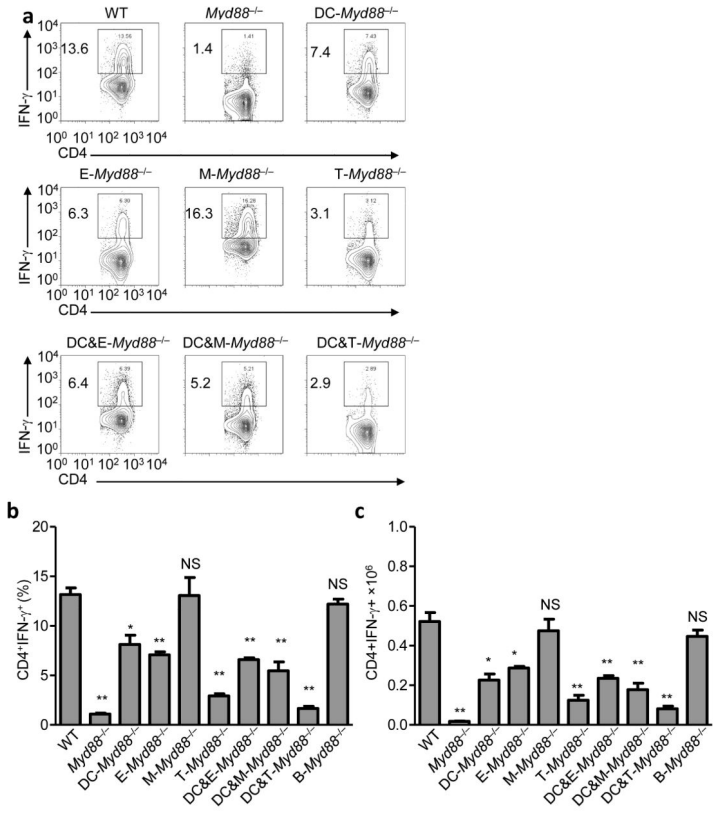

Figure 6. Intrinsic T-cell MyD88 signaling regulates T_H1 polarization

(**a**) WT, *Myd88*$^{-/-}$, and mice with cell type-specific inactivation of MyD88 in DCs, epithelial cells (E), macrophages (M), T cells (T), DCs and epithelial cells (DC&E), DCs and macrophages (DC&M), and DCs and T cells (DC&T) were infected orally with 20 cysts per mouse of the ME49 strain of *T. gondii.* Mesenteric lymph nodes (mLNs) were harvested on day 7 post-infection, and IFN-γ production by CD4$^+$ T cells was analyzed by flow cytometry. The data shown are representative of five independent experiments each involving 4–6 mice per group. (**b**) Average frequency and (**c**) absolute quantification of T_H1 cells (CD4$^+$IFN-γ$^+$) in the mLNs of mice infected orally with the parasite. The data shown are representative of five independent experiments each involving 4–6 mice per group. * P< 0.01; ** P< 0.001.

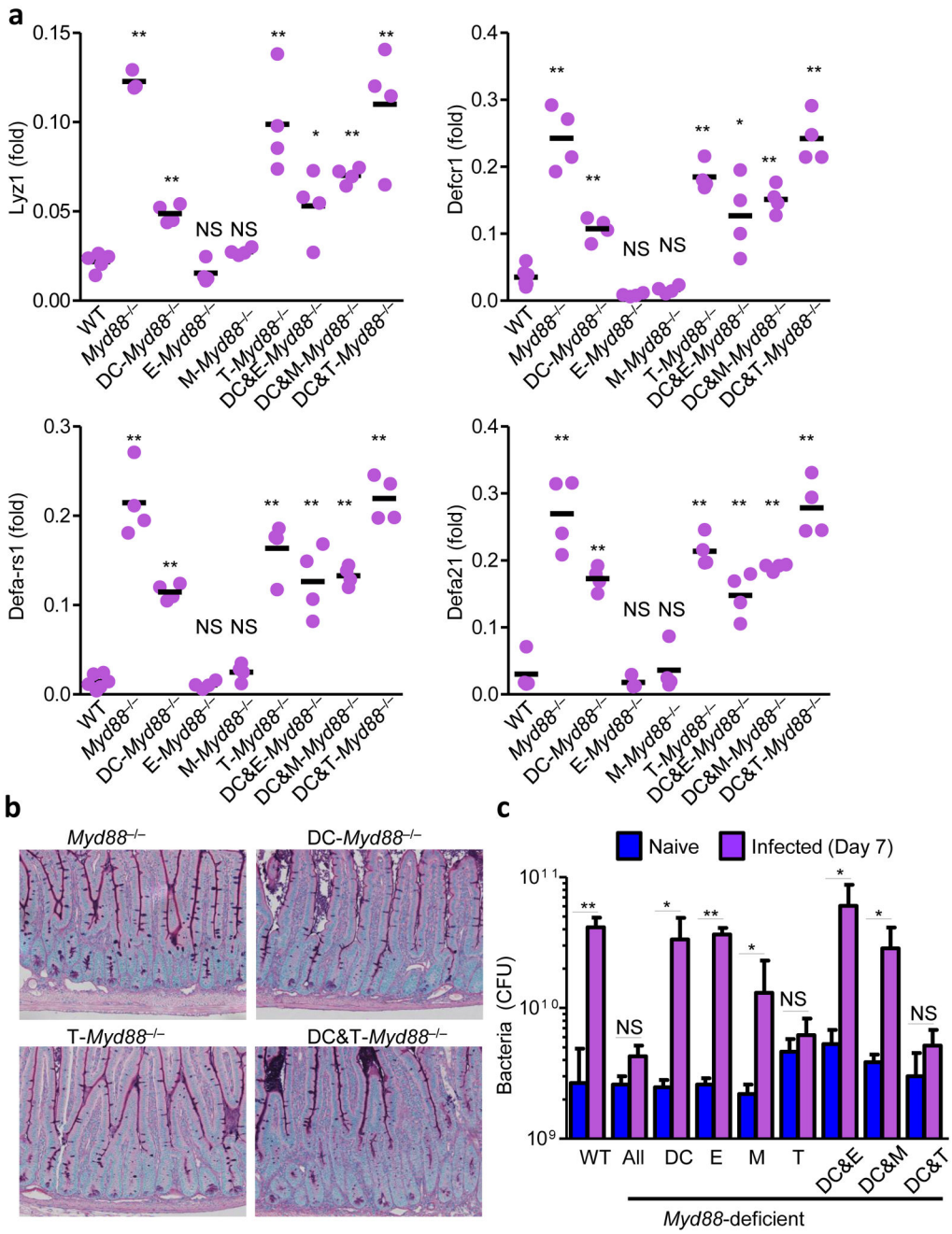

Figure 7. Intrinsic T-cell MyD88 signaling mediates loss of Paneth cells intestinal dysbiosis

(**a**) qRT-PCR analysis of relative expression of Lyz1, Defcr1 (alpha-defensin-1), Defa-rs1, Defa21 in the small intestines of WT, *Myd88*$^{-/-}$, and cell type-specific MyD88-deficient mice on day 7 post-infection. The results are representative of five independent experiments each involving 4–5 mice per group. (**b**) Histological visualization of Paneth cells in small intestines of DC-Myd88$^{-/-}$, T-*Myd88*$^{-/-}$, and DC&T-*Myd88*$^{-/-}$ mice compared to complete MyD88-deficient mice (*Myd88*$^{-/-}$). The results are representative of five independent experiments each involving 4–5 mice per group. (**c**) Bacterial loads in the lumens of small intestines of naïve (blue) or infected WT, *Myd88*$^{-/-}$ and cell type-specific *Myd88*$^{-/-}$ mice

(purple) were analyzed by plating bacteria on blood agar plates on day 7 post-infection. * P< 0.05; ** P< 0.01. The results are representative of five independent experiments each involving 4–5 mice per group.